

Photonic crystals of shape-anisotropic colloidal particles

Krassimir P. Velikov^{a)}

Soft Condensed Matter, Debye Institute, Utrecht University, Princetonlaan 5, 3584 CC Utrecht, The Netherlands

Teun van Dillen and Albert Polman

FOM Institute for Atomic and Molecular Physics, Kruislaan 407, 1098 SJ Amsterdam, The Netherlands

Alfons van Blaaderen^{b)}

Soft Condensed Matter, Debye Institute, Utrecht University, Princetonlaan 5, 3584 CC Utrecht, The Netherlands and FOM Institute for Atomic and Molecular Physics, Kruislaan 407, 1098 SJ Amsterdam, The Netherlands

(Received 8 February 2002; accepted for publication 3 June 2002)

Spherical silica (SiO_2), zinc sulfide (ZnS), and core-shell particles of these materials undergo substantial anisotropic plastic deformation under high-energy ion irradiation. Individual particles can be turned into oblate or prolate ellipsoids with exact control over the aspect ratio. In this letter, we report on the fabrication and optical characterization of thin three-dimensional photonic crystals of spherical particles, which have been anisotropically deformed into spheroidal oblates by means of ion irradiation. As a result of the collective deformation process, both the unit cell symmetry and the particle form factor have been changed leading to appreciable tunability in the optical properties of the photonic crystal. © 2002 American Institute of Physics. [DOI: 10.1063/1.1497197]

Since their discovery, photonic crystals (materials with a periodically modulated dielectric constant) have received considerable attention because of their unique ability to control the propagation and spontaneous emission of light.¹⁻³ For photonic crystals (PC) with a high enough contrast in combination with a certain symmetry, the propagation of electromagnetic waves can be inhibited for a certain frequency range leading to the formation of a photonic band gap (PBG). PCs are expected to have many applications such as filters, optical switches, and low-threshold lasers.⁴ The fabrication of PCs with a submicron periodicity, however, is difficult and requires state-of-the-art microlithography techniques. With their ability to self-organize into three-dimensional (3D) structures with different symmetries colloidal spheres offer an alternative way for the fabrication of PCs at optical wavelengths.^{5,6}

It is well known that face-centered cubic (fcc) PCs made of dielectric spheres do not possess a 3D PBG,⁷⁻⁹ because of a symmetry-induced degeneracy of the polarization modes at the W point of the Brillouin zone. This degeneracy can be broken by using shape-anisotropic¹⁰ or dielectrically anisotropic¹¹ objects as building blocks. Here also, non-spherical colloidal particles offer excellent possibilities as building blocks to create PCs. However, there are additional difficulties to overcome in comparison to the conventional spherical particles.¹² First, there are not many methods to synthesize nonspherical colloids with well-defined size and shapes.¹³ Second, most of these particles (e.g., metal oxides) strongly absorb light in the visible region. Finally, the most commonly used methods for assembling, such as controlled

drying¹⁴ and sedimentation,¹⁵ might not be suitable in the case of nonspherical particles or will provide less control over the final structure.

Recently, it was demonstrated that inorganic, amorphous, and polycrystalline, spherical colloidal particles can be turned into ellipsoids by high-energy ion irradiation.^{16,17} The method allows continuous variation of the particle shape from oblate to prolate ellipsoids with precise control over the aspect ratio. PCs built from ellipsoidal particles can be used as templates to make inverse opals.^{6,18} Because of the shape anisotropy, there will be strong polarization effects leading to birefringence at long wavelengths.¹⁰ The ability to change the shape of the unit cell and its contents will allow control over polarization modes in a PC.¹⁹

In this letter, we demonstrate the fabrication of photonic crystals of (almost) ellipsoidal colloidal particles obtained after ion irradiation of colloidal crystals of spherical SiO_2 and ZnS -core- SiO_2 -shell²⁰ particles. We performed angle-resolved optical transmission measurements on thin photonic crystals. We show that as a result of the irradiation, both the shape of the individual particles and the lattice spacing in the original fcc (111) direction were changed leading to a substantial shift in the position of the stop gap.

Colloidal PCs were fabricated from monodisperse SiO_2 and ZnS -core- SiO_2 -shell^{20,21} spheres. Silica particles with a radius of 110 nm (relative width in the size distribution, $\delta = 3\%$) were synthesized using a microemulsion method followed by seeded growth.²² ZnS -core- SiO_2 -shell particles with a total radius of 128 nm ($\delta = 5\%$) with a ZnS - SiO_2 composite core radius of 84 nm ($\delta = 6\%$) were prepared as described elsewhere.²⁰ Thin colloidal crystals of eight to ten layers thick were grown on clean glass substrates using a controlled drying method.^{14,20,23} With this method, the fcc crystals are uniquely oriented with the lines of touching particles forming the (111) plane parallel to the drying front.²⁴

^{a)}Author to whom correspondence should be addressed; electronic mail: k.p.velikov@phys.uu.nl

^{b)}Author to whom correspondence should be addressed; electronic mail: a.vanblaaderen@phys.uu.nl

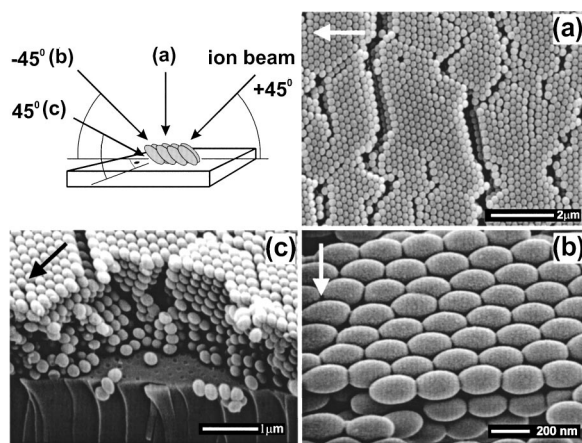


FIG. 1. SEM images of a planar photonic crystal of close-packed SiO_2 oblate ellipsoids obtained after irradiation with 4 MeV Xe^{4+} ions to a fluence of $1.0 \times 10^{15} \text{ cm}^{-2}$ at angle of 45° at 90 K. (a) Top view of the crystal showing the (111)-crystal plane. (b) Top view at -45° (perpendicular to the plane of irradiation) of the crystal. The average semi-axes of the ellipsoids determined from the SEM picture are $x = 123 \pm 5 \text{ nm}$ and $y = 74 \pm 2 \text{ nm}$. (c) Side view of a broken crystal showing the depth of the deformation caused by the irradiation. The big arrows show the direction of the ion beam.

Silica crystals were annealed at 600°C for 4 h in air.²⁵ Colloidal crystals were irradiated with 4 MeV Xe^{4+} ions at 90 K with the sample surface held at an angle of 45° with respect to the direction of the ion beam. The ion fluence was 4.0×10^{14} and $1.0 \times 10^{15} \text{ cm}^{-2}$ for ZnS-core- SiO_2 -shell and SiO_2 , respectively. Samples were coated with a 5 nm Pt/Pd layer before analyzing by scanning electron microscopy (SEM) at 5 kV. The angle-resolved optical transmission spectra were measured with a Cary 500 UV-near-IR spectrometer. The light beam spot diameter was about 5 mm^2 , which is comparable to the area of single-crystalline domains for a crystal before annealing or irradiation.

Figure 1 shows SEM micrographs of a thin planar crystal of close-packed monodisperse silica colloidal particles. After the irradiation all particles were deformed and turned into (almost) oblate ellipsoids.¹⁶ The particles expanded relatively undisturbed in the plane perpendicular to the plane of irradiation. A deformation in other directions, e.g., along the (111) direction (crystallographic directions mentioned hereafter are with respect to the undeformed fcc crystal), will lead to a more complex collective deformation. The collective deformation process preserved the 3D order of the crystal. The cracks parallel to the direction of irradiation formed because of shrinking of the film and stress that results from the attachment of the colloidal crystal to the substrate. We have found after the optical measurements were performed that free-standing colloidal crystalline films do not crack. All ellipsoids formed are oriented with longitudinal axes in a plane parallel to the plane of ion irradiation, i.e., 45° with respect to the glass substrate. When the sample is imaged at -45° [Fig. 1(b)] both semi-axes (x, y) can be measured directly. The ellipsoidal semi-axes $x = 123 \pm 5 \text{ nm}$ and $y = 74 \pm 2 \text{ nm}$ (aspect ratio 1.65 ± 0.09) were determined by image processing of the SEM micrographs. From the side view [Fig. 1(c)], one can see that the anisotropic deformation is extended throughout the full crystal including to the first layer of particles in contact with the substrate. However, as the crystal thickness ($\sim 1.8 \mu\text{m}$) is close to the calculated

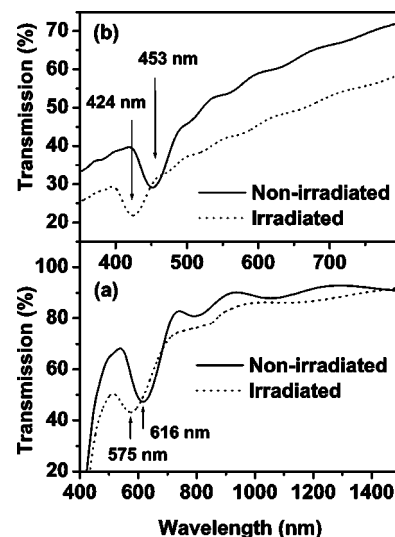


FIG. 2. Optical transmission spectra taken along the (111) crystallographic axis measured on thin colloidal photonic crystals of (a) ZnS-core- SiO_2 -shell and (b) SiO_2 colloidal particles grown on glass substrates. The position of the minimum in the optical transmission spectra of the irradiated samples (dotted line) is shifted to shorter wavelengths in comparison to the nonirradiated samples (solid line). The crystals consist of ten layers of close-packed silica particles (b) and eight layers of core-shell particles (a), respectively. In both cases a shift of $>20 \text{ nm}$ in the position of the stop gap is observed.

penetration depth of the 4 MeV Xe^{4+} ions, taking the angle of irradiation and the filling fraction of SiO_2 into account, it might be that the particles close to the substrate are slightly less deformed. Higher energies can be used to deform thicker crystals. From Fig. 1(c), it is apparent that there is a slight deviation from the ellipsoidal shape caused by the fact that deforming spheres were touching each other in the crystal. Most likely, this increases the packing fraction and consequently the effective refractive index of the composite.

Figure 2 shows optical transmission spectra of thin photonic crystals of SiO_2 [Fig. 2(a)] and ZnS-core- SiO_2 -shell [Fig. 2(b)] colloidal particles taken along the (111) direction. The spectra before and after the ion irradiation exhibit a minimum in the optical transmission, where the Bragg condition is fulfilled and light is diffracted away from the axis of propagation. The presence of a Bragg peak after irradiation indicates that the crystal structure remains after the ion irradiation. However, the minimum, which corresponds to the stop gap, has shifted to shorter wavelengths both in Figs. 2(a) and 2(b). This shift is an effect of the changed lattice spacing in the crystal and possibly a small densification of the whole crystal. Figure 3 shows optical transmission spectra measured at different angles on nonirradiated and irradiated samples. The transmission was measured from different points on the $L \rightarrow W$ line toward the Γ of the Brillouin zone. In both cases, the stop gap gradually disappears at large angles of incidence.

In order to determine the correct position of the stop gap from the experimental spectra, we subtracted the background scattering.^{20,26} The positions of the stop gaps for irradiated and nonirradiated crystals as a function of $\sin^2(\theta)$ are shown in Fig. 4. In the case of spherical particles, the position of the stop gap can, to a first approximation, be related to the particle diameter, $2R$, and the effective dielectric constant of the medium through the modified Bragg law, λ_{max}

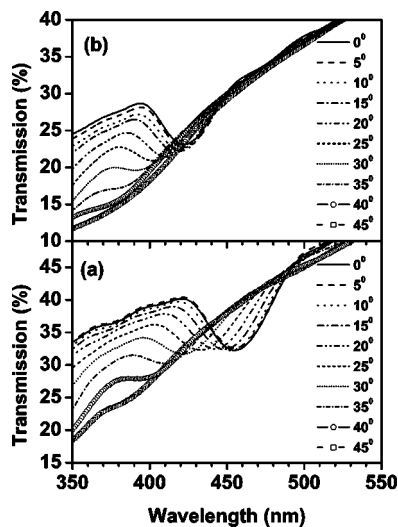


FIG. 3. Angle-resolved optical transmission spectra of colloidal photonic crystals of silica particles grown on a glass substrate. The spectra were taken from different points on the $L \rightarrow W$ line towards the Γ point of the Brillouin zone. (a) Nonirradiated crystal of spherical particles. (b) Irradiated crystal of oblate ellipsoidal particles of aspect ratio 1.65 ± 0.09 .

$= 2d_{111} \sqrt{\varepsilon_{\text{eff}} - \varepsilon_b \sin^2 \theta}$, where $d_{111} = 2R\sqrt{2/3}$ is the distance between the crystal planes in the (111) direction, ε_{eff} is the volume averaged dielectric constant of the composite: $\varepsilon_{\text{eff}} = f\varepsilon_p + (1-f)\varepsilon_b$, where f is the crystal filling fraction ($f = 0.74$ for closely packed spheres), ε_p and ε_b are the dielectric constants of the particle, and the background, respectively. From the fit with a silica refractive index of 1.47, we determined a particle radius of 103 nm ($d_{111} = 168$ nm). This value corresponds to a $\sim 6\%$ shrinkage of the silica particles after thermal annealing and is similar as observed before.²⁵ The calculated volume of the spheres before the irradiation agrees well with the volume of an ellipsoid ($4/3\pi x^2 y$) calculated using the values of the two semi-axes determined from the SEM images. The volume of a single silica particle was previously found not to change significantly after ion irradiation.¹⁶

After the ion irradiation, the lattice spacing in the (111) direction decreased. As a result, the position of the Bragg peak shifted accordingly to shorter wavelengths. Because of the deformation, the crystal unit cell is now tetragonal rather

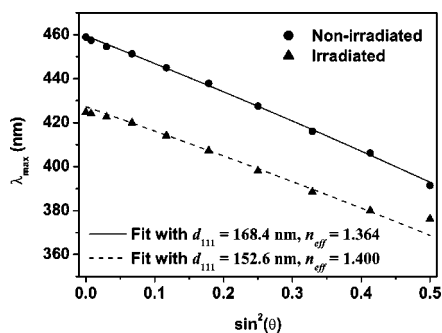


FIG. 4. Position of the transmission minima in Fig. 3 as a function of $\sin^2(\theta)$. After irradiation, the positions of the stop gap for ellipsoidal particles (triangles) shift to shorter wavelengths in comparison to the case of spherical particles (circles). The values are determined from the experimental spectra after correction for the background scattering. The lines are the theoretical fits using $\lambda_{\text{max}} = 2d_{111} \sqrt{\varepsilon_{\text{eff}} - \sin^2 \theta}$.

than cubic. It can be shown that the lattice spacing in the (111) direction after isotropic deformation under certain angle, α , can be written as $d_{111} = 2y\sqrt{2/3}[1 - (1 - y^2/x^2)\cos^2 \alpha]^{-1/2}$, where x and y are the lengths of the two semi-axes of the ellipsoid ($x > y$). Using this equation, we find $d_{111} = 147$ which is close to the value of $d_{111} = 153$ nm determined from the fit in Fig. 4. This analysis assumes that the particles deform into ellipsoids and there is no change in the volume of the particles. From the fit in Fig. 4, we also determined an effective refractive index of the composite of 1.40, which corresponds to a $\sim 2.6\%$ increase in comparison to the nonirradiated sample. This indicates that some densification of the crystal has taken place after the irradiation assuming that the dielectric constant of silica did not change.

In conclusion, we demonstrated the fabrication of colloidal photonic crystals of shape-anisotropic particles from crystals made of spheres using MeV ion irradiation. In this way, both the lattice structure and the form factor were changed in a controlled way. The aspect ratio of the shape-anisotropic particles can be used as an additional parameter to engineer the PBGs.

The authors thank D. A. Mazurenko and A. Imhof (Utrecht University) for helpful discussions, and J. Hoogenboom (AMOLF) for the preparation of the free-standing crystals. This work is part of the research program of the "Stichting voor Fundamenteel Onderzoek der Materie," which is financially supported by the "Nederlandse Organisatie voor Wetenschappelijk Onderzoek."

¹V. P. Bykov, Sov. J. Quantum Electron. **4**, 861 (1975).

²E. Yablonovitch, Phys. Rev. Lett. **58**, 2059 (1987).

³S. John, Phys. Rev. Lett. **58**, 2486 (1987).

⁴C. M. Soukoulis, *Photonic Crystals and Light Localization in the 21st Century*, in NATO Science series, Series C Vol. C 563 (Kluwer, Dordrecht, 2001).

⁵A. van Blaaderen, MRS Bull. **23**, 39 (1998).

⁶V. L. Colvin, MRS Bull. **26**, 637 (2001).

⁷K. M. Leung and Y. F. Liu, Phys. Rev. Lett. **65**, 2646 (1990).

⁸H. S. Sozuer, J. W. Haus, and R. Inguva, Phys. Rev. B **45**, 13962 (1992).

⁹J. W. Haus, J. Mod. Opt. **41**, 195 (1994).

¹⁰J. W. Haus, H. S. Sozuer, and R. Inguva, J. Mod. Opt. **39**, 1991 (1992).

¹¹Z. Y. Li, J. Wang, and B. Y. Gu, Phys. Rev. B **58**, 3721 (1998).

¹²Y. Lu, Y. D. Yin, and Y. N. Xia, Adv. Mater. **13**, 415 (2001).

¹³E. Matijevic, Chem. Mater. **5**, 412 (1993).

¹⁴P. Jiang, J. F. Bertone, K. S. Hwang, and V. L. Colvin, Chem. Mater. **11**, 2132 (1999).

¹⁵R. Mayoral, J. Requena, J. S. Moya, C. Lopez, A. Cintas, H. Miguez, F. Meseguer, L. Vazquez, M. Holgado, and A. Blanco, Adv. Mater. **9**, 257 (1997).

¹⁶E. Snoeks, A. van Blaaderen, T. van Dillen, C. M. van Kats, M. L. Brongersma, and A. Polman, Adv. Mater. **12**, 1511 (2000).

¹⁷T. van Dillen, A. Polman, W. Fukarek, and A. van Blaaderen, Appl. Phys. Lett. **78**, 910 (2001).

¹⁸O. D. Velev and E. W. Kaler, Adv. Mater. **12**, 531 (2000).

¹⁹S. Noda, M. Yokoyama, M. Imada, A. Chutinan, and M. Mochizuki, Science **293**, 1123 (2001).

²⁰K. P. Velikov, A. Moroz, and A. van Blaaderen, Appl. Phys. Lett. **80**, 49 (2002).

²¹K. P. Velikov and A. van Blaaderen, Langmuir **17**, 4779 (2001).

²²K. Osseasare and F. J. Arriagada, Colloids Surface **50**, 321 (1990).

²³N. D. Denkov, O. D. Velev, P. A. Kralchevsky, I. B. Ivanov, H. Yoshimura, and K. Nagayama, Langmuir **8**, 3183 (1992).

²⁴K. P. Velikov, C. G. Christova, R. P. A. Dullens, and A. van Blaaderen, Science **296**, 106 (2002).

²⁵H. Miguez, F. Meseguer, C. Lopez, A. Blanco, J. S. Moya, J. Requena, A. Mifsud, and V. Fornes, Adv. Mater. **10**, 480 (1998).

²⁶J. F. Bertone, P. Jiang, K. S. Hwang, D. M. Mittleman, and V. L. Colvin, Phys. Rev. Lett. **83**, 300 (1999).